

# Soft Pilot Reuse and Multicell Block Diagonalization Precoding for Massive MIMO Systems

Xudong Zhu, Zhaocheng Wang, *Senior Member, IEEE*, Chen Qian, Linglong Dai, *Senior Member, IEEE*,  
Jinhui Chen, Sheng Chen, *Fellow, IEEE*, and Lajos Hanzo, *Fellow, IEEE*

**Abstract**—The users at cell edge of a massive multiple-input–multiple-output (MIMO) system suffer from severe pilot contamination (PC), which leads to poor quality of service (QoS). To enhance the QoS for these edge users, soft pilot reuse (SPR) combined with multicell block diagonalization (MBD) precoding is proposed. Specifically, the users are divided into two groups according to their large-scale fading coefficients, which are referred to as the center users, who only suffer from modest PC, and the edge users, who suffer from severe PC. Based on this distinction, the SPR scheme is proposed for improving the QoS for the edge users, whereby a cell-center pilot group is reused for all cell-center users in all cells, whereas a cell-edge pilot group is applied for the edge users in the adjacent cells. By extending the classical block diagonalization precoding to a multicell scenario, the MBD precoding scheme projects the downlink transmit signal onto the null space of the subspace spanned by the intercell channels of the edge users in adjacent cells. Thus, the intercell interference contaminating the edge users’ signals in the adjacent cells can be efficiently mitigated, and hence, the QoS of these edge users can be further enhanced. Our theoretical analysis and simulation results demonstrate that both the uplink and downlink rates of the edge users are significantly improved, albeit at the cost of the slightly decreased rate of center users.

**Index Terms**—Intercell interference (ICI), massive multiple-input–multiple-output (MIMO) system, multicell block diagonalization (MBD) precoding, pilot contamination (PC), quality of service (QoS), soft pilot reuse (SPR).

## I. INTRODUCTION

**I**N an effort to meet the escalating demand for increasingly higher capacity and improved-reliability wireless systems,

Manuscript received December 15, 2014; revised April 28, 2015; accepted June 9, 2015. Date of publication June 17, 2015; date of current version May 12, 2016. This work was supported in part by the Beijing Natural Science Foundation under Grant 4142027; by the National High Technology Research and Development Program of China under Grant 2014AA01A704; by the National Nature Science Foundation of China under Grant 61271266; by the Foundation of Shenzhen Government; and by the Information Technology Development Division, Sony Corporation and Sony China Research Laboratory, Sony (China) Ltd. The review of this paper was coordinated by Dr. X. Dong.

X. Zhu, Z. Wang, C. Qian, and L. Dai are with the Tsinghua National Laboratory for Information Science and Technology (TNList), Department of Electronic Engineering, Tsinghua University, Beijing 100084, China (e-mail: zhuxd12@mails.tsinghua.edu.cn; zcwang@tsinghua.edu.cn; qianc10@mails.tsinghua.edu.cn; dail@tsinghua.edu.cn).

J. Chen is with Sony China Research Laboratory, Beijing 100190, China (e-mail: jinhui.chen@sony.com.cn).

S. Chen is with Electronics and Computer Science, University of Southampton, Southampton SO17 1BJ, U.K., and also with King Abdulaziz University, Jeddah 21589, Saudi Arabia (e-mail: sqc@ecs.soton.ac.uk).

L. Hanzo is with Electronics and Computer Science, University of Southampton, Southampton SO17 1BJ, U.K. (e-mail: lh@ecs.soton.ac.uk).

Color versions of one or more of the figures in this paper are available online at <http://ieeexplore.ieee.org>.

Digital Object Identifier 10.1109/TVT.2015.2445795

the “massive” or large-scale multiple-input–multiple-output (LS-MIMO) concept has been proposed [1]–[3], where, typically, each base station (BS) is equipped with a large number of antenna elements (AEs) to serve far fewer single-AE users. This way, each user may have access to several AEs. This LS-MIMO technology offers several significant advantages in comparison with the conventional MIMO concept having a moderate number of AEs. First, asymptotic analysis based on random matrix theory [2] demonstrates that both the intracell interference and the uncorrelated noise effects can be efficiently mitigated, as the number of AEs tends to infinity. Furthermore, the energy consumption of cellular BSs can be substantially reduced [4], and the LS-MIMO systems are robust, since the failure of one or a few of the AEs and radio-frequency chains would not appreciably affect the resultant system performance [1]. Additionally, low-complexity signal processing relying on matched filter (MF)-based transmit precoding (TPC) and detection can be used for approaching the optimal performance, when the number of AEs at the BS tends to infinity [2].

Similar to conventional MIMO systems, knowledge of the channel state information (CSI) is also required at the BS of LS-MIMO systems, namely, for data detection in the uplink (UL) and for multiuser TPC in the downlink (DL) [2], [5]. In the time-division duplexing (TDD) protocol, the BS estimates the UL channels and obtains the DL CSI by exploiting the channel’s reciprocity [1], [3], [6]. However, this approach suffers from the so-called pilot contamination (PC) problem [1]–[3] in multicell multiuser scenarios due to the reuse of the pilot sequences in adjacent cells, which imposes grave interference on the channel estimate at the BS. Furthermore, the commonly used MF and zero-forcing (ZF) TPC schemes will impose intercell interference (ICI) on the DL transmission, which cannot be reduced by increasing the number of AEs at the BS.

Hence, the problems of ICI and PC have been extensively studied [7]–[21]. The fractional frequency reuse (FFR) scheme [7], [8] adopted in LTE Release 9 aims for mitigating the ICI by assigning orthogonal frequency bands to edge users in the adjacent cells at the cost of additional spectral resources. The original frequency-division duplexing (FDD)-based coordinated multipoint (CoMP) transmission of LTE-A Release 11 [9] is able to avoid the ICI between adjacent cells, whereby each user estimates and feeds back the quantized DL channel from all adjacent cells to the corresponding BS, and then, the BS distributes the CSI to adjacent cells. However, this kind of FDD-based CoMP technique would not be feasible for massive MIMO since the CSI feedback overhead would be huge as the

number of BS antennas increases [10]. Using time-shifted pilot sequences for asynchronous transmission among the adjacent cells [11], [12] partially mitigates this problem, but it leads to mutual interference between data transmission and pilot transmission. A TPC scheme can be used for mitigating the ICI with the aid of joint multicell processing [13], [14] but, again, imposes a high information exchange overhead. In [15], specific conditions on the channel's covariance matrix were imposed, which is only valid for the asymptotic case of infinitely many AEs at the BS. The angle of arrival (AOA)-based methods of [16] and [17] exploit the fact that the users having mutually nonoverlapping AOAs hardly contaminate each other even if they use the same pilot sequence, but naturally, the efficiency of these methods relies on the assumption that the AOA spread of each user is small, which is not always the case under realistic channel conditions. A data-aided channel estimation scheme was proposed in [18], whereby partially decoded data are used for estimating the channel, and the PC effects can be beneficially reduced by iterative processing at the cost of an increased computational complexity. Additionally, the blind method of [19] and [20] based on subspace partitioning is capable of reducing the ICI under the assumption that the channel vectors of different users are orthogonal, which is not often the case in practice. The scheme proposed in [21] is capable of eliminating PC altogether, but this is achieved with the aid of a complex DL and UL training procedure. Note that all these existing contributions treat all users in the same way, as though they suffer from the same PC, but in reality, the severity of PC varies among the users.

Against the preceding background, inspired by the FFR scheme [7] adopted in LTE Release 9, we propose a soft pilot reuse (SPR) scheme for mitigating the PC of LS-MIMO systems, whereby a cell-edge pilot group is applied for the cell-edge users in adjacent cells, whereas the cell-center users reuse the same center pilot group in all cells. Furthermore, by extending the classical block diagonalization (BD) precoding [23] to a multicell scenario, a multicell block diagonalization (MBD) TPC technique is conceived for mitigating the ICI and for enhancing the quality of service (QoS) for the edge users. Specifically, the contributions of this paper are summarized as follows.

- We break away from the traditional practice of treating the PC for all users identically—instead, we divide the users into two different groups to be considered separately, namely, center users subjected to a slight PC and the edge users suffering from more severe PC. This way, the center users can benefit directly from the LS-MIMO technology, and the efforts can be directed toward improving the QoS for the edge users.
- In contrast to the FFR scheme, which assigns orthogonal frequency bands to the edge users in adjacent cells, the proposed SPR scheme divides the pilot types into two groups within the same frequency band, i.e., in a center pilot group, which is reused for the center users in all cells, and in an edge pilot group, which is applied for the edge users in adjacent cells. Thus, for the edge users, the accuracy of the channel estimation is improved,

and the UL achievable rate is increased. Moreover, by using slightly more pilot resources for edge users, the BS becomes capable of estimating not only the intracell channels of the users within the reference cell but the knowledge of the “intercell channels” of the edge users in the adjacent cells as well.

- Different from the original CoMP technique that has to obtain the intercell channels by consuming large overhead [9], [10], the proposed MBD precoding can directly exploit the partial knowledge of the intercell channels and is capable of suppressing the ICI imposed on the edge users of the adjacent cells. Specifically, by extending the classical BD TPC to a multicell scenario, the MBD TPC projects the DL transmit signal onto the null space of the subspace spanned by the partially known intercell channels. Thus, the ICI imposed on the edge users of the adjacent cells can be substantially mitigated; hence, the QoS of the edge users is significantly enhanced.
- To analyze the performance of our proposal, we compare the associated pilot requirements, derive the attainable average UL and DL rates, and characterize the computational complexity imposed. Our theoretical derivation confirms that both the achievable UL and DL rates of the edge users are significantly improved at the cost of requiring slightly more pilots. Moreover, our simulation results show that the average UL and DL cell throughputs in the SPR- and MBD-aided system are able to approach and even exceed that of the conventional system, provided that a modestly increased number of BS AEs are affordable.

The rest of this paper is organized as follows. In Section II, we briefly review the multicell LS-MIMO system model, whereas Section III is devoted to detailing the PC, which is the main performance-limiting factor of LS-MIMO systems. Section IV further details the motivation of this paper, whereas the proposed SPR scheme and the MBD precoding are discussed in Section V. Section VI provides our performance analysis of the proposed SPR scheme and MBD precoding. Our simulation results quantifying the benefits of our proposals are presented in Section VII, whereas our conclusions follow in Section VIII.

Throughout our discussions, boldface lower and uppercase symbols represent vectors and matrices, respectively. The transpose, conjugate, and Hermitian transpose operators are given by  $(\cdot)^T$ ,  $(\cdot)^*$ , and  $(\cdot)^H$ , respectively. The Moore–Penrose pseudoinverse operator is denoted by  $(\cdot)^\dagger$ , and the trace operator is represented by  $\text{Tr}(\cdot)$ , whereas  $\text{diag}\{a_1, a_2, \dots, a_m\}$  denotes the diagonal matrix associated with  $a_1, a_2, \dots, a_m$  at its diagonal entries, and the  $M \times M$  identity matrix is given by  $\mathbf{I}_M$ . The number of elements in a set is denoted by  $\text{card}\{\cdot\}$ , and the  $l_p$  norm is denoted by  $\|\cdot\|_p$ , whereas the expectation operator is given by  $\text{E}\{\cdot\}$ .

## II. SYSTEM MODEL

A multicell multiuser LS-MIMO system is illustrated in Fig. 1, which is composed of  $L$  hexagonal cells, each having a central BS associated with  $M$  antennas to serve  $K$  ( $K \ll M$ )

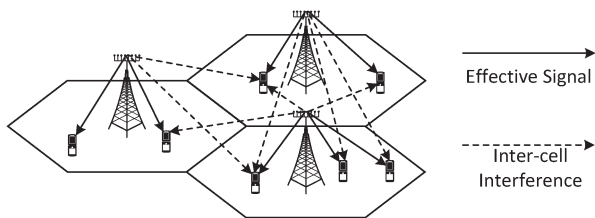


Fig. 1. Multiuser multicell LS-MIMO system.

single-antenna users [1], [2]. The channel vector  $\mathbf{h}_{i,j,k} \in \mathbb{C}^{M \times 1}$  of the link spanning from the  $k$ th user of the  $j$ th cell to the BS of the  $i$ th cell can be formulated as

$$\mathbf{h}_{i,j,k} = \mathbf{g}_{i,j,k} \sqrt{\beta_{i,j,k}}. \quad (1)$$

The small-scale fading vectors  $\mathbf{g}_{i,j,k} \in \mathbb{C}^{M \times 1}$  are statistically independent for the  $K$  users, and they obey the complex-valued Gaussian distribution having a zero-mean vector and a covariance matrix  $\mathbf{I}_M$ ; hence, we have  $\mathbf{g}_{i,j,k} \sim \mathcal{CN}(\mathbf{0}, \mathbf{I}_M)$ . Still referring to (1), the large-scale fading coefficients  $\beta_{i,j,k}$  are the same for the different antennas at the same BS, but they are user dependent. Moreover, they are related to both the path loss and shadow fading, which will be addressed in detail in the context of our simulations. Thus, the channel matrix of all the  $K$  users in the  $j$ th cell and the BS in the  $i$ th cell can be represented by

$$\begin{aligned} \mathbf{H}_{i,j} &= [\mathbf{h}_{i,j,1} \ \mathbf{h}_{i,j,2}, \dots, \mathbf{h}_{i,j,K}] \\ &= [\mathbf{g}_{i,j,1} \ \mathbf{g}_{i,j,2}, \dots, \mathbf{g}_{i,j,K}] \mathbf{D}_{i,j}^{\frac{1}{2}} \end{aligned} \quad (2)$$

where  $\mathbf{D}_{i,j} = \text{diag}(\beta_{i,j,1}, \beta_{i,j,2}, \dots, \beta_{i,j,K})$  denotes the large-scale fading matrix relating all the  $K$  users in the  $j$ th cell to the  $i$ th cell's BS.

By adopting the TDD protocol, the BS obtains the DL channel estimate by exploiting the reciprocity of the UL and DL channels. More specifically, both the small-scale fading vectors and the large-scale fading coefficients may be deemed to be equal for both the DL and UL directions, provided that the bandwidth is sufficiently narrow for avoiding the independent fading of the DL and the UL.

Before considering the PC phenomenon, we summarize the asymptotic orthogonality on random vector [1]. Let  $\mathbf{x}, \mathbf{y} \in \mathbb{C}^{M \times 1}$  be two independent vectors with distribution  $\mathcal{CN}(\mathbf{0}, c\mathbf{I}_M)$ . Then, from the law of large numbers, we have

$$\lim_{M \rightarrow \infty} \frac{\mathbf{x}^H \mathbf{x}}{M} \xrightarrow{\text{a.s.}} c, \quad \lim_{M \rightarrow \infty} \frac{\mathbf{x}^H \mathbf{y}}{M} \xrightarrow{\text{a.s.}} 0 \quad (3)$$

where  $\xrightarrow{\text{a.s.}}$  denotes the almost sure convergence.

### III. PILOT CONTAMINATION

By considering the TDD protocol, we adopt the widely used block-fading channel model, whereby the channel vectors  $\mathbf{h}_{i,j,k}$  remain constant during the channel's coherence interval. As shown in Fig. 2, each coherence interval is composed of four

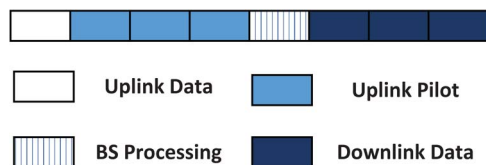


Fig. 2. Multiuser multicell MIMO TDD protocol.

stages for each user [12]: 1) UL data transmission; 2) UL pilot transmission; 3) BS processing; and 4) DL data transmission.

At the first stage, all users in all cells synchronously send UL data to their corresponding BSs, and the user data received at the BS in the  $i$ th cell can be represented as  $\mathbf{y}_i^u = \sqrt{\rho_u} \sum_{j=1}^L \sum_{k=1}^K \mathbf{h}_{i,j,k} x_{j,k}^u + \mathbf{n}_i^u$ , where  $x_{j,k}^u$  with  $E\{|x_{j,k}^u|^2\} = 1$  denotes the symbol transmitted from the  $k$ th user roaming in the  $j$ th cell,  $\rho_u$  represents the UL data transmission power, and  $\mathbf{n}_i^u \in \mathbb{C}^{M \times 1}$  denotes the corresponding UL channel's additive Gaussian white noise (AWGN) vector associated with  $E\{\mathbf{n}_i^u (\mathbf{n}_i^u)^H\} = (\sigma_n^u)^2 \mathbf{I}_M$ .

For a typical LS-MIMO system, the pilot sequences used within a specific cell are orthogonal, but the same pilot group is typically reused in the adjacent cells due to the limited number of orthogonal pilot sequences. Thus, during the second stage, the matrix of pilot sequences received at the BS of the  $i$ th cell, which is denoted by  $\mathbf{Y}_i^p \in \mathbb{C}^{M \times \tau}$ , can be represented as  $\mathbf{Y}_i^p = \sqrt{\rho_p} \sum_{j=1}^L \mathbf{H}_{i,j} \mathbf{\Phi} + \mathbf{N}_i^p$ , where the matrix  $\mathbf{\Phi} = [\phi_1 \ \phi_2, \dots, \phi_K]^T \in \mathbb{C}^{K \times \tau}$  containing the transmitted pilot sequence satisfies  $\mathbf{\Phi} \mathbf{\Phi}^H = \mathbf{I}_K$ ,  $\rho_p$  is the transmission power of the pilots, and  $\mathbf{N}_i^p \in \mathbb{C}^{M \times \tau}$  denotes the UL channel's AWGN matrix.

During the third stage, the BS of the  $i$ th cell obtains an estimate of the channel matrix  $\mathbf{H}_{i,i}$  using any conventional channel estimation method by directly correlating the received pilot matrix with the local pilot matrix, yielding

$$\hat{\mathbf{H}}_{i,i} = \frac{1}{\sqrt{\rho_p}} \mathbf{Y}_i^p \mathbf{\Phi}^H = \mathbf{H}_{i,i} + \sum_{j \neq i} \mathbf{H}_{i,j} + \frac{1}{\sqrt{\rho_p}} \mathbf{N}_i^p \mathbf{\Phi}^H. \quad (4)$$

It can readily be seen that the channel estimate of the  $k$ th user in the  $i$ th cell, namely,  $\hat{\mathbf{h}}_{i,i,k}$ , is a linear combination of the channels  $\mathbf{h}_{i,j,k}$  for  $1 \leq j \leq L$ , which include the channels of the users in the other cells associated with the same pilot sequence. This phenomenon is referred to as PC [1]–[3]. Given the estimated channel matrix  $\hat{\mathbf{H}}_{i,i}$  and by adopting the low-complexity MF detector, the detected symbol arriving from the  $k$ th user in the  $i$ th cell can be represented as

$$\begin{aligned} \hat{x}_{i,k}^u &= \hat{\mathbf{h}}_{i,i,k}^H \mathbf{y}_i^u \\ &= \sqrt{\rho_u} \left( \mathbf{h}_{i,i,k}^H \mathbf{h}_{i,i,k} x_{i,k}^u + \sum_{j \neq i} \mathbf{h}_{i,j,k}^H \mathbf{h}_{i,j,k} x_{j,k}^u \right) + \varepsilon_{i,k} \\ &\stackrel{(a)}{\approx} M \sqrt{\rho_u} \left( \beta_{i,i,k} x_{i,k}^u + \sum_{j \neq i} \beta_{i,j,k} x_{j,k}^u \right) \end{aligned} \quad (5)$$

where  $\mathbf{v}_{i,k}$  denotes the  $k$ th column of  $(1/\sqrt{\rho_p})\mathbf{N}_i^p\Phi^H$ ,  $\varepsilon_{i,k}^u$  represents the interference, which can be reduced to an arbitrarily low level by increasing the number of transmit antennas  $M$  at the BS, and  $\stackrel{(a)}{\approx}$  indicates that the approximation holds by invoking the asymptotic orthogonality associated with  $M \rightarrow \infty$ . Thus, the UL signal-to-interference-plus-noise ratio (SINR) of the  $k$ th user in the  $i$ th cell can be calculated as

$$\text{SINR}_{i,k}^u = \frac{|\mathbf{h}_{i,i,k}^H \mathbf{h}_{i,i,k}|^2}{\sum_{j \neq i} |\mathbf{h}_{i,j,k}^H \mathbf{h}_{i,j,k}|^2 + |\varepsilon_{i,k}^u|^2 / \rho_u} \stackrel{(a)}{\approx} \frac{\beta_{i,i,k}^2}{\sum_{j \neq i} \beta_{i,j,k}^2} \quad (6)$$

and the achievable UL rate can be expressed as  $C_{i,k}^u = (1 - \mu)E\{\log_2(1 + \text{SINR}_{i,k}^u)\}$ , where  $0 < \mu < 1$  evaluates the spectral efficiency reduction caused by the pilot transmission [24]. It is clear that the UL achievable rate remains limited by the PC and it cannot be increased by simply assigning an increased transmission power and/or pilot power, i.e., by increasing  $\rho_u$  and/or  $\rho_p$ .

The PC affects the DL transmission during the fourth stage as well. The normalized MF precoding matrix [3] is commonly used for the DL transmission, which can be represented by  $\mathbf{W}_i = (1/\sqrt{\gamma_i})\hat{\mathbf{H}}_{i,i}^*$ , where  $\gamma_i = \text{Tr}(\hat{\mathbf{H}}_{i,i}^T \hat{\mathbf{H}}_{i,i}^*)/K$  is a normalization factor. The BS in the  $i$ th cell transmits an  $M$ -dimensional signal vector as  $\mathbf{s}_i^d = \mathbf{W}_i \mathbf{x}_i^d$ , where  $\mathbf{x}_i^d = [x_{i,1}^d, x_{i,2}^d, \dots, x_{i,K}^d]^T$  with  $E\{|x_{i,k}^d|^2\} = 1$  denotes the source symbol vector for the  $K$  users in the  $i$ th cell. The received signals of the  $K$  users in the  $i$ th cell can be collected together as  $\mathbf{y}_i^d = \sqrt{\rho_d} \sum_{j=1}^L \mathbf{H}_{j,i}^T (1/\sqrt{\gamma_j}) \hat{\mathbf{H}}_{j,j}^* \mathbf{x}_j^d + \mathbf{n}_i^d$ , where  $\mathbf{n}_i^d$  denotes the DL channel AWGN vector associated with  $E\{\mathbf{n}_i^d (\mathbf{n}_i^d)^H\} = (\sigma_n^d)^2 \mathbf{I}_M$ . Similar to the derivation shown in (6), the DL SINR of the  $k$ th user in the  $i$ th cell can be derived as

$$\text{SINR}_{i,k}^d = \frac{|\mathbf{h}_{i,i,k}^T \mathbf{h}_{i,i,k}^*|^2}{\sum_{j \neq i} |\mathbf{h}_{j,i,k}^T \mathbf{h}_{j,i,k}^*|^2 + |\varepsilon_{i,k}^d|^2 / \rho_d} \stackrel{(a)}{\approx} \frac{\beta_{i,i,k}^2}{\sum_{j \neq i} \beta_{j,i,k}^2} \quad (7)$$

where  $\varepsilon_{i,k}^d$  denotes the corresponding interference similar to  $\varepsilon_{i,k}^u$  given in (5). The corresponding DL rate can be represented as  $C_{i,k}^d = (1 - \mu)E\{\log_2(1 + \text{SINR}_{i,k}^d)\}$ .

In summary, the PC caused by the reuse of the same orthogonal pilot group in adjacent cells cannot be reduced by increasing the number of antennas at the BS; hence, it limits the achievable performance of multicell multiuser LS-MIMO systems.

#### IV. MOTIVATION OF OUR PROPOSAL

In the existing state-of-the-art solutions [7], [8], [11]–[21], which aim for reducing the PC, all users are treated identically. However, according to (6) and (7), it becomes clear that the attainable SINR is proportional to the large-scale fading coef-

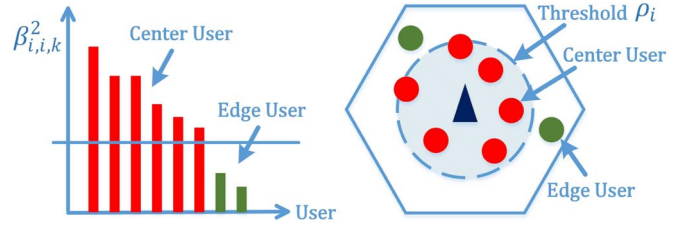


Fig. 3. Illustrative example of the user division.

ficients  $\beta_{i,i,k}^2$ , which are different for the  $K$  users of each cell. Thus, we have to break away from this traditional concept of treating the PC for all users identically, which motivates our idea of dividing the users of each cell into two groups, namely, the group of center users subjected to modest PC and the group of edge users suffering from severe PC. We will treat them differently.

In fact, the limit of the UL SINR of the  $k$ th user in the  $i$ th cell, which is defined by

$$\eta_{i,k} = \frac{\beta_{i,i,k}^2}{\sum_{j \neq i} \beta_{i,j,k}^2} \quad (8)$$

specifies the severity of the PC for this user. Therefore, it is easy to sort the users in a cell according to their SINR values  $\eta_{i,k}$ , if all the large-scale fading coefficients  $\{\beta_{i,j,k}^2\}$  are known at the BS, which is a key assumption stipulated in the state-of-the-art contributions [6], [11], [18]. However, in practice, it is difficult for the BS to obtain an accurate estimate of the large-scale fading coefficients of the users in other cells, i.e., of  $\beta_{i,j,k}^2$  for  $j \neq i$ , unless BS cooperation is invoked, which is typically associated with a substantial side-information overhead.

Since we have  $\eta_{i,k} \propto \beta_{i,i,k}^2$ , we may also use  $\beta_{i,i,k}^2$  for estimating the severity of the PC for the  $k$ th user roaming in the  $i$ th cell. In contrast to  $\beta_{i,j,k}^2$  for  $j \neq i$ , all the large-scale fading coefficients  $\{\beta_{i,i,k}^2\}$  of the  $K$  users in the  $i$ th cell can be readily obtained. Thus, the  $K$  users in the  $i$ th cell can be readily divided into two groups according to

$$\beta_{i,i,k}^2 > \rho_i \rightarrow \begin{cases} \text{Yes} \rightarrow \text{center users} \\ \text{No} \rightarrow \text{edge users.} \end{cases} \quad (9)$$

The user-grouping threshold  $\rho_i$  can be set to

$$\rho_i = \frac{\lambda}{K} \sum_{k=1}^K \beta_{i,i,k}^2 \quad (10)$$

where  $\lambda$  can be adjusted according to the specific system configuration. A simple case is illustrated in Fig. 3, where, according to the large-scale fading coefficients  $\{\beta_{i,i,k}^2\}$  and the given threshold  $\rho_i$ , the users are divided into two groups, namely, the center users associated with only a slight PC and the edge users subjected to severe PC. Note that the threshold  $\rho_i$  is not based on the geographic locations of the users—it is rather based on the signal space of  $\{\beta_{i,i,k}^2\}$ .

Since the center users only suffer from minor PC, the conventional LS-MIMO scheme outlined earlier is capable of attaining a high performance. By contrast, the edge users suffer from

serious PC; hence, their performance based on the conventional LS-MIMO scheme is expected to be poor. To enhance the QoS of the edge users, who suffer from heavy PC, we propose the more sophisticated SPR scheme and MBD precoding in the following.

### V. PROPOSED SOFT PILOT REUSE SCHEME AND MULTICELL BLOCK DIAGONALIZATION PRECODING

Based on the division of users into two groups as outlined in Section IV, it is plausible that the center users indeed benefit from the conventional LS-MIMO technique. By contrast, improved measures have to be considered for enhancing the QoS of the edge users, such as our SPR and MBD schemes, which will be discussed in detail in the following.

#### A. Proposed Soft Pilot Reuse Scheme

Inspired by the FFR scheme, which assigns orthogonal frequency bands to edge users in adjacent cells to prevent serious ICI in 3GPP LTE Release 9, we propose the SPR scheme to mitigate the PC, whereby orthogonal pilot subgroups are assigned to the edge users in the adjacent cells, whereas a center pilot group is reused for the center users of all cells.

More specifically, consider a typical LS-MIMO system, which is composed of  $L$  hexagonal cells, where the  $i$ th cell supports  $K_i$  users. In the conventional LS-MIMO scheme [1]–[3], the number of orthogonal pilot sequences required can be calculated as

$$K_{CS} = \max\{K_i, i = 1, 2, \dots, L\}. \quad (11)$$

In contrast to the conventional LS-MIMO scheme, where all users are treated identically, the  $K_i$  users of the  $i$ th cell are first divided into two groups according to their large-scale fading coefficients  $\{\beta_{i,i,k}^2\}$ , which have cardinalities of

$$K_i = K_{i,c} + K_{i,e} \quad (12)$$

where  $K_{i,c} = \text{card}\{k : \beta_{i,i,k}^2 > \rho_i\}$  denotes the number of center users, whereas  $K_{i,e} = \text{card}\{k : \beta_{i,i,k}^2 \leq \rho_i\}$  represents the number of edge users. Thus, the number of orthogonal pilot sequences needed in the proposed SPR scheme can be calculated as

$$K_{SPR} = K_c + K_e \quad (13)$$

where  $K_c = \max\{K_{i,c}, i = 1, 2, \dots, L\}$  denotes the number of pilot sequences assigned to the center users, whereas  $K_e = \sum_{i=1}^L K_{i,e}$  denotes the number of pilot sequences dedicated to the edge users. It should be pointed out that we assume having  $L$  cooperating cells; thus,  $L$  is a moderate value. For example, we have  $L = 7$  for the classic seven-cell system. Then, the entire set of pilot resources  $\Phi_{SPR} \in \mathbb{C}^{K_{SPR} \times \tau}$  associated with  $\Phi_{SPR} \Phi_{SPR}^H = \mathbf{I}_{K_{SPR}}$  can be divided into

$$\Phi_{SPR} = [\Phi_c^T \ \Phi_e^T]^T \quad (14)$$

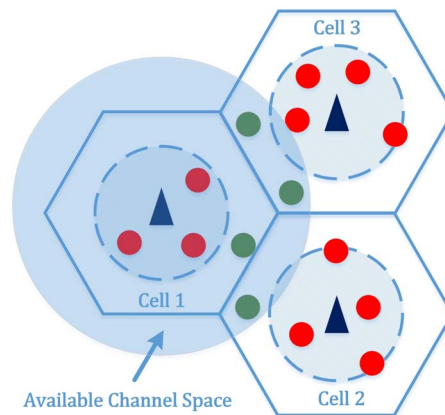


Fig. 4. Example of the proposed SPR scheme.

where  $\Phi_c \in \mathbb{C}^{K_c \times \tau}$  is reused for the center users in all cells, and  $\Phi_e \in \mathbb{C}^{K_e \times \tau}$  is applied to the edge users of the adjacent cells. Furthermore,  $\Phi_e$  can be divided into  $L$  partitions, as

$$\Phi_e = [\Phi_{e,1}^T \ \Phi_{e,2}^T \ \dots \ \Phi_{e,L}^T]^T \quad (15)$$

where  $\Phi_{e,i} \in \mathbb{C}^{K_{i,e} \times \tau}$  is applied to the  $K_{i,e}$  edge users in the  $i$ th cell. Thus, the pilot sequences applied to edge users are orthogonal to those of the other users roaming in the adjacent cells.

In the example in Fig. 4, there are three hexagonal cells associated with  $K_1 = 4$ ,  $K_2 = 5$ , and  $K_3 = 6$  users. To completely eliminate the PC would require 15 orthogonal pilot sequences. It can be readily calculated that we have  $K_{CS} = 6$  and  $K_{SPR} = 8$  for this simple case. Although the proposed SPR scheme requires slightly more pilot resources than the conventional scheme, the QoS of the edge users can be significantly improved, which will be verified in the following.

#### B. Channel Estimation Based on Soft Pilot Reuse

By applying the proposed SPR scheme, the BS becomes capable of estimating the channels for its edge users in the absence of PC, since the pilot sequences assigned to the edge users are all orthogonal. Moreover, the BS can also obtain the partial knowledge of the intercell channels of the edge users in adjacent cells, which is the dominant source of the ICI inflicted upon these edge users of the adjacent cells during the BS’s DL transmissions.

Specifically, we consider the same LS-MIMO system as in Section V-A, which is composed of  $L$  hexagonal cells, where the  $i$ th cell has  $K_i$  users. Based on the proposed SPR scheme, we divide the channel matrix  $\mathbf{H}_{i,j}$  as defined in (2) into two parts, i.e.,

$$\mathbf{H}_{i,j} \rightarrow [\mathbf{H}_{i,j}^c \ \mathbf{H}_{i,j}^e] \quad (16)$$

where  $\mathbf{H}_{i,j}^c \in \mathbb{C}^{M \times K_{j,c}}$  denotes the channel matrix of the link spanning from the center users in the  $j$ th cell to the BS in the  $i$ th cell, whereas  $\mathbf{H}_{i,j}^e \in \mathbb{C}^{M \times K_{j,e}}$  denotes the channel matrix of the link spanning from the edge users in the  $j$ th cell to the

BS in the  $i$ th cell. Then, the pilot sequence received at the BS of the  $i$ th cell can be represented by

$$\bar{\mathbf{Y}}_i^p = \sqrt{\rho_p} \left( \sum_{j=1}^L \mathbf{H}_{i,j}^c \Phi_c(r : K_{j,c}) + \sum_{j=1}^L \mathbf{H}_{i,j}^e \Phi_{e,j} \right) + \bar{\mathbf{N}}_i^p \quad (17)$$

where  $\Phi_c(r : K_{j,c})$  denotes the submatrix composed of the first  $K_{j,c}$  rows of  $\Phi_c$ , whereas  $\bar{\mathbf{N}}_i^p$  denotes the corresponding AWGN matrix at the UL receiver.

Then, the BS becomes capable of estimating the channel of its center users as

$$\begin{aligned} \hat{\mathbf{H}}_{i,i}^c &= \frac{1}{\sqrt{\rho_p}} \bar{\mathbf{Y}}_i^p \Phi_c^H(r : K_{i,c}) \\ &= \mathbf{H}_{i,i}^c + \sum_{j \neq i} \mathbf{H}_{i,j}^c(c : K_{i,c}) + \bar{\mathbf{N}}_i^c \end{aligned} \quad (18)$$

where  $\bar{\mathbf{N}}_i^c = (1/\sqrt{\rho_p}) \bar{\mathbf{N}}_i^p \Phi_c^H(r : K_{i,c})$ , which can be reduced to an arbitrarily small value by increasing  $M$ , and  $\mathbf{H}_{i,j}^c(c : K_{i,c})$  denotes the matrix composed of the first  $K_{i,c}$  columns of  $\mathbf{H}_{i,j}^c$ . Note that, if we have  $K_{i,c} > K_{j,c}$ , then  $K_{i,c} - K_{j,c}$  zero vectors are used to fill  $\mathbf{H}_{i,j}^c(c : K_{i,c})$ . In contrast to the conventional scheme of (4), the proposed scheme only allows the center users to reuse the same pilot group of  $\Phi_c$ , since the PC imposed on these center users is modest. Consequently, the severity of the PC inflicted upon the channel estimation of the center users given in (18) is minor.

On the other hand, by adopting the proposed SPR scheme, the BS of the  $i$ th cell becomes capable of acquiring the channel estimate of its edge users without excessive PC, yielding

$$\hat{\mathbf{H}}_{i,i}^e = \frac{1}{\sqrt{\rho_p}} \bar{\mathbf{Y}}_i^p \Phi_{e,i}^H = \mathbf{H}_{i,i}^e + \bar{\mathbf{N}}_i^e \quad (19)$$

where we have  $\bar{\mathbf{N}}_i^e = (1/\sqrt{\rho_p}) \bar{\mathbf{N}}_i^p \Phi_{e,i}^H$ , which can be made arbitrarily small by increasing the number of antennas at the BS. It is clear that the PC is completely eliminated for these edge users, and therefore, the channel estimation accuracy of these edge users is significantly enhanced. By contrast, with the conventional scheme, these edge users suffer from grave PC, and hence, their channel estimates have extremely poor quality, which severely limits the achievable UL detection performance. With the aid of the proposed SPR scheme, the full channel estimate at the BS of the  $i$ th cell is then given by

$$\hat{\mathbf{H}}_{i,i} = \begin{bmatrix} \hat{\mathbf{H}}_{i,i}^c & \hat{\mathbf{H}}_{i,i}^e \end{bmatrix} \quad (20)$$

which is significantly more accurate than that of the conventional channel estimation scheme of (4). Thus, given this more accurate channel estimate, the UL achievable rate of the edge users can be significantly increased, which will be analyzed in detail in Section VI.

Moreover, since the edge users of the adjacent cells rely on orthogonal pilot sequences, a BS can also acquire the partial intercell channels for the edge users of the adjacent cells. Specifically, by correlating the received pilot matrix  $\bar{\mathbf{Y}}_i^p$  with  $\Phi_{e,j}$ , the BS of the  $i$ th cell becomes capable of acquiring the

partial intercell channels from the edge users in the  $j$ th cell without PC, as follows:

$$\hat{\mathbf{H}}_{i,j}^e = \frac{1}{\sqrt{\rho_p}} \bar{\mathbf{Y}}_i^p \Phi_{e,j}^H = \mathbf{H}_{i,j}^e + \bar{\mathbf{N}}_{i,j}^e, \quad j \neq i \quad (21)$$

where  $\bar{\mathbf{N}}_{i,j}^e = (1/\sqrt{\rho_p}) \bar{\mathbf{N}}_i^p \Phi_{e,j}^H$  can be rendered arbitrarily small upon increasing  $M$ . Thus, the BS of the  $i$ th cell becomes capable of accurately estimating all the partial intercell channels of the links spanning from the edge users of the adjacent cells, which comprises an estimate of the intercell channel matrix  $\mathbf{A}_i \in \mathbb{C}^{(K_e - K_{i,e}) \times M}$  as

$$\hat{\mathbf{A}}_i = \left[ \hat{\mathbf{H}}_{i,1}^e, \dots, \hat{\mathbf{H}}_{i,i-1}^e \hat{\mathbf{H}}_{i,i+1}^e, \dots, \hat{\mathbf{H}}_{i,L}^e \right]^T. \quad (22)$$

For instance, in the simple example depicted in Fig. 4, the BS in the first cell is able to acquire the accurate channel estimates of both its edge user and of the partial intercell channels of the edge users in two adjacent cells. The intercell channel matrix  $\mathbf{A}_i$  provides important information for the DL TPC design. Armed with its accurate estimate  $\hat{\mathbf{A}}_i$ , the BS of the  $i$ th cell will be able to beneficially preprocess its transmissions for the sake of reducing the ICI inflicted upon its neighboring edge users roaming in the adjacent cells, which is the topic in the following.

### C. Multicell Block Diagonalization Precoding

By selecting the TPC vector for a specific user from the null space spanned by the channels of other users, the classical BD TPC scheme [23] adopted in single-cell multiuser MIMO systems is capable of eliminating the multiuser interference. Armed with the estimate of the partial intercell channels, we propose the MBD TPC by extending the classical BD TPC to a multicell multiuser scenario. Specifically, by projecting the DL transmit signal onto the null space of the subspace spanned by the intercell channels, the proposed MBD TPC becomes capable of eliminating the ICI imposed on these edge users.

To obtain the null space of the intercell channels, we first apply the classic singular value decomposition (SVD) [22] to the intercell channel matrix  $\hat{\mathbf{A}}_i$ , yielding

$$\hat{\mathbf{A}}_i = \mathbf{U}_i \Sigma_i \mathbf{V}_i^H \quad (23)$$

where  $\mathbf{U}_i \in \mathbb{C}^{(K_e - K_{i,e}) \times (K_e - K_{i,e})}$  denotes the left singular vector matrix,  $\mathbf{V}_i \in \mathbb{C}^{M \times M}$  denotes the right singular vector matrix, and  $\Sigma_i \in \mathbb{C}^{(K_e - K_{i,e}) \times M}$  is composed of the singular values as

$$\Sigma_i = \begin{bmatrix} \hat{\Sigma}_i & \mathbf{0}_{r_i \times (M - r_i)} \\ \mathbf{0}_{(K_e - K_{i,e} - r_i) \times r_i} & \mathbf{0}_{(K_e - K_{i,e} - r_i) \times (M - r_i)} \end{bmatrix} \quad (24)$$

in which  $r_i = \text{rank}(\hat{\mathbf{A}}_i)$  is the rank of  $\hat{\mathbf{A}}_i$ ,  $\hat{\Sigma}_i = \text{diag}\{\sigma_{i,1}, \sigma_{i,2}, \dots, \sigma_{i,r_i}\}$ , and the singular values satisfy

$$\sigma_{i,1} \geq \sigma_{i,2} \geq \dots \geq \sigma_{i,r_i} > 0. \quad (25)$$

According to the properties of full SVD, the null space of the intercell channels, namely,  $\text{Null}(\hat{\mathbf{A}}_i) \subseteq \mathbb{C}^M$ , can be spanned

by the columns of the matrix  $\mathbf{B}_i \in \mathbb{C}^{M \times (M-r_i)}$ , which is a submatrix of  $\mathbf{V}_i$  defined by

$$\mathbf{B}_i = [\mathbf{v}_{i,r_i+1} \ \mathbf{v}_{i,r_i+2} \ \cdots \ \mathbf{v}_{i,M}] \quad (26)$$

where  $\mathbf{v}_{i,j}$  denotes the  $j$ th column of  $\mathbf{V}_i$ . Note that the existence of this null space is guaranteed owing to the fact that the number of antennas at the BS of LS-MIMO systems is much larger than that of the edge users, i.e., we have

$$M \gg K_e \geq K_e - K_{i,e} \geq r_i. \quad (27)$$

The large null space of the intercell channels indicates that, for any TPC matrix chosen from this null space, i.e.,  $\forall \mathbf{W}_i \subset \text{Null}(\hat{\mathbf{A}}_i)$ , we have

$$\hat{\mathbf{A}}_i \mathbf{W}_i = \mathbf{0} \Rightarrow \left( \hat{\mathbf{H}}_{i,j}^e \right)^T \mathbf{W}_i = \mathbf{0} \quad \forall j \neq i \quad (28)$$

which means that this TPC matrix calculated for the  $i$ th cell is capable of eliminating the ICI inflicted upon the edge users roaming in the adjacent cells. It is plausible, however, that a precoding matrix, which is randomly chosen from the null space  $\text{Null}(\hat{\mathbf{A}}_i)$  may cause severe intracell interference. To avoid the deleterious effects of intracell interference, we project a conventional TPC matrix onto this null space.

For example, by projecting this conventional MF precoding matrix  $\mathbf{W}_i^{\text{MF}} = (1/\sqrt{\gamma_i^{\text{MF}}}) \hat{\mathbf{H}}_{i,i}^*$  onto the null space  $\text{Null}(\hat{\mathbf{A}}_i)$ , we can generate the MF-based MBD matrix as

$$\mathbf{W}_i^{\text{MFMBD}} = \frac{1}{\sqrt{\gamma_i^{\text{MFMBD}}}} \mathbf{P}_{\mathbf{B}_i} \hat{\mathbf{H}}_{i,i}^* \quad (29)$$

where  $\mathbf{P}_{\mathbf{B}_i} = \mathbf{B}_i \mathbf{B}_i^\dagger$  denotes the projection operator based on the matrix  $\mathbf{B}_i$ , and  $\gamma_i^{\text{MFMBD}}$  is a normalization factor given by

$$\begin{aligned} \gamma_i^{\text{MFMBD}} &= \frac{1}{K_i} \text{Tr} \left( \hat{\mathbf{H}}_{i,i}^T \mathbf{P}_{\mathbf{B}_i} \mathbf{P}_{\mathbf{B}_i} \hat{\mathbf{H}}_{i,i}^* \right) \\ &= \frac{1}{K_i} \text{Tr} \left( \hat{\mathbf{H}}_{i,i}^T \mathbf{P}_{\mathbf{B}_i} \hat{\mathbf{H}}_{i,i}^* \right) \end{aligned} \quad (30)$$

in which  $\mathbf{P}_{\mathbf{B}_i}^H = \mathbf{P}_{\mathbf{B}_i}$  and  $\mathbf{P}_{\mathbf{B}_i} \mathbf{P}_{\mathbf{B}_i} = \mathbf{P}_{\mathbf{B}_i}$  are applied.

Similarly, by projecting the conventional ZF TPC matrix onto the null space  $\text{Null}(\hat{\mathbf{A}}_i)$ , we can generate the ZF-based MBD matrix as

$$\begin{aligned} \mathbf{W}_i^{\text{ZFMDBD}} &= \frac{1}{\sqrt{\gamma_i^{\text{ZFMDBD}}}} \left( \left( \mathbf{P}_{\mathbf{B}_i}^* \hat{\mathbf{H}}_{i,i} \right)^T \right)^\dagger \\ &= \frac{1}{\sqrt{\gamma_i^{\text{ZFMDBD}}}} \mathbf{P}_{\mathbf{B}_i} \hat{\mathbf{H}}_{i,i}^* \left( \hat{\mathbf{H}}_{i,i}^T \mathbf{P}_{\mathbf{B}_i} \mathbf{P}_{\mathbf{B}_i} \hat{\mathbf{H}}_{i,i}^* \right)^{-1} \\ &= \frac{1}{\sqrt{\gamma_i^{\text{ZFMDBD}}}} \mathbf{P}_{\mathbf{B}_i} \hat{\mathbf{H}}_{i,i}^* \left( \hat{\mathbf{H}}_{i,i}^T \mathbf{P}_{\mathbf{B}_i} \hat{\mathbf{H}}_{i,i}^* \right)^{-1} \end{aligned} \quad (31)$$

where the normalization factor  $\gamma_i^{\text{ZFMDBD}}$  is calculated as

$$\begin{aligned} \gamma_i^{\text{ZFMDBD}} &= \frac{1}{K_i} \text{Tr} \left( \hat{\mathbf{H}}_{i,i}^T \mathbf{P}_{\mathbf{B}_i} \mathbf{P}_{\mathbf{B}_i} \hat{\mathbf{H}}_{i,i}^* \right)^{-1} \\ &= \frac{1}{K_i} \text{Tr} \left( \hat{\mathbf{H}}_{i,i}^T \mathbf{P}_{\mathbf{B}_i} \hat{\mathbf{H}}_{i,i}^* \right)^{-1}. \end{aligned} \quad (32)$$

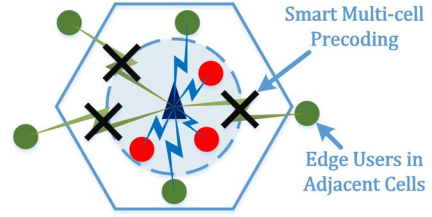


Fig. 5. Illustrative example of the MBD precoding scheme.

Both the precoding matrices  $\mathbf{W}_i^{\text{MFMBD}}$  and  $\mathbf{W}_i^{\text{ZFMDBD}}$  are capable of eliminating the ICI imposed on the edge users of the adjacent cells. An illustrative example is depicted in Fig. 5, where, based on the proposed SPR scheme, the BS becomes capable of estimating the partial intercell channels of the edge users roaming in the adjacent cells. The MBD TPC then projects the DL transmission signal onto the null space of the partial intercell channels to eliminate the ICI contaminating the reception of these edge users in the adjacent cells. Therefore, the MBD TPC significantly increases the DL achievable rate of edge users, and consequently, the QoS of edge users is considerably enhanced.

## VI. PERFORMANCE ANALYSIS

Before we investigate the performance of the proposed SPR and MBD schemes, we first discuss the amount of pilot resources required, then derive both the UL and DL achievable rates, and, finally, consider the computational complexity imposed.

### A. Pilot Resource Consumption

As seen in (11), the conventional scheme requires  $K_{\text{CS}} = \max\{K_i, 1 \leq i \leq L\}$  number of orthogonal pilot sequences, and it suffers from grave PC. Again, to eliminate the PC caused by the reuse of the same pilot group in adjacent cells, the most plausible solution is to apply orthogonal pilot sequences to all users in all cells. However, the number of orthogonal pilot sequences would be increased to

$$K_{\text{OS}} = \sum_{i=1}^L K_i \quad (33)$$

which leads to a substantial spectral efficiency reduction.

Recall that the proposed SPR and MBD schemes are capable of enhancing the QoS for edge users at the expense of a slightly increased number of pilot resources. More specifically, by comparing (11) and (13), the additional pilot resources required by the proposed SPR scheme can be derived as

$$K_{\text{SPR}} - K_{\text{CS}} = \sum_{i \neq i_0} K_{i,e} \leq \sum_{i=1}^L K_{i,e} \quad (34)$$

where  $i_0$  denotes the index of the cell that has the most users, i.e.,  $K_{i_0} = K_{\text{CS}}$ . It is clear that the additional number of pilot sequences is close to the total number of the edge users. Since the edge users are classified according to the threshold  $\rho_i$ , which can be adjusted by the parameter  $\lambda$ , the number of edge users can be also flexibly adjusted.

More explicitly, the careful choice of the parameter  $\lambda$  provides a flexible tradeoff between the pilot resources required and the achievable system performance of the proposed SPR scheme. At one extreme end, when the parameter  $\lambda$  is set to 0, all the users will be regarded as edge users, and the proposed SPR scheme becomes equivalent to the orthogonal scheme, where all users in all cells use orthogonal pilot sequences. Naturally, this achieves the best performance but relies on the most pilot resources, requiring  $K_{OS}$  orthogonal pilot sequences. At the other extreme, when the parameter  $\lambda$  is set to a sufficiently large value, e.g.,  $\lambda = K_{CS}$ , then all users are regarded as center users, and the proposed SPR scheme degrades to the conventional scheme that reuses the same pilot group in all cells. Hence, the resultant arrangement attains the worst performance but consumes the minimum pilot resources, hence requiring only  $K_{CS}$  orthogonal pilot sequences.

### B. Uplink Transmission

For the center users, the average SINR performance of SPR-aided UL transmission becomes almost the same as that of applying the conventional scheme. This is because, for the center users in a cell, the estimated channel matrix of (4) obtained by applying the conventional scheme is very similar to that of (18) obtained by applying the SPR scheme. However, the achievable rate of the center users of the SPR-aided UL transmission is slightly reduced, since the pilot overhead increases, i.e.,  $\mu \rightarrow (K_{SPR}/K_{CS})\mu$ . On the other hand, the performance of UL transmission for the edge users is much more complex, as shown in the following.

Similar to the received signal given in Section III based on the conventional scheme, the received signal at the BS of the  $i$ th cell based on the SPR scheme can be represented as

$$\bar{\mathbf{y}}_i^u = \sqrt{\rho_u} \sum_{j=1}^L (\mathbf{H}_{i,j}^c \mathbf{x}_j^{u,c} + \mathbf{H}_{i,j}^e \mathbf{x}_j^{u,e}) + \bar{\mathbf{n}}_i^u \quad (35)$$

where  $\mathbf{x}_j^{u,c} = [x_{j,1}^{u,c}, x_{j,2}^{u,c}, \dots, x_{j,K_{j,c}}^{u,c}]^T$  denotes the symbol vector transmitted from the  $K_{j,c}$  center users in the  $j$ th cell,  $\mathbf{x}_j^{u,e} = [x_{j,1}^{u,e}, x_{j,2}^{u,e}, \dots, x_{j,K_{j,e}}^{u,e}]^T$  is the symbol vector transmitted from the  $K_{j,e}$  edge users in the  $j$ th cell, and  $\bar{\mathbf{n}}_i^u$  denotes the corresponding UL AWGN vector.

By adopting the MF detector based on the channel estimation obtained by the SPR scheme for the edge users in the  $i$ th cell, i.e.,  $\hat{\mathbf{H}}_{i,i}^e$  of (19), the detected symbol vector for the  $K_{i,e}$  users in the  $i$ th cell is given by

$$\begin{aligned} \hat{\mathbf{x}}_i^{u,e} &= (\hat{\mathbf{H}}_{i,i}^e)^H \bar{\mathbf{y}}_i^u \\ &= (\mathbf{H}_{i,i}^e + \bar{\mathbf{N}}_i^e)^H \left( \sqrt{\rho_u} \sum_{j=1}^L (\mathbf{H}_{i,j}^c \mathbf{x}_j^{u,c} + \mathbf{H}_{i,j}^e \mathbf{x}_j^{u,e}) + \bar{\mathbf{n}}_i^u \right) \\ &= \sqrt{\rho_u} (\mathbf{H}_{i,i}^e)^H \mathbf{H}_{i,i}^e \mathbf{x}_i^{u,e} + \boldsymbol{\eta}_i^{u,e} \stackrel{(a)}{\approx} M \sqrt{\rho_u} \mathbf{D}_{i,i}^e \mathbf{x}_i^{u,e} \end{aligned} \quad (36)$$

where  $\mathbf{D}_{i,i}^e = \text{diag}\{\beta_{i,i,1}^e, \beta_{i,i,2}^e, \dots, \beta_{i,i,K_{i,e}}^e\}$  denotes the sub-diagonal matrix of  $\mathbf{D}_{i,i}^e$  consisting of the  $K_{i,e}$  edge users' large-

scale fading coefficients, and  $\boldsymbol{\eta}_i^{u,e} = [\eta_{i,1}^{u,e}, \eta_{i,2}^{u,e}, \dots, \eta_{i,K_{i,e}}^{u,e}]^T$  denotes the interference, which can be made arbitrarily small by increasing the number of antennas at the BS. In particular, for the  $k$ th edge user in the  $i$ th cell, the detected symbol is given by

$$\begin{aligned} \hat{x}_{ik}^{u,e} &= \sqrt{\rho_u} (\mathbf{h}_{i,i,k}^e)^H \mathbf{h}_{i,i,k}^e x_{i,k}^{u,e} + \mu_{i,k}^{u,e} + \eta_{i,k}^{u,e} \\ &\stackrel{(a)}{\approx} M \sqrt{\rho_u} \beta_{i,i,k}^e x_{i,k}^{u,e} \end{aligned} \quad (37)$$

where  $\mu_{i,k}^{u,e} = \sqrt{\rho_u} \sum_{k' \neq k} (\mathbf{h}_{i,i,k'}^e)^H \mathbf{h}_{i,i,k}^e x_{i,k'}^{u,e}$  is the intracell interference arriving from the other edge users in the same cell, which can be rendered arbitrarily small by increasing  $M$ . Similar to the derivation in (6), the UL SINR of the  $k$ th edge user in the  $i$ th cell can be calculated as

$$\overline{\text{SINR}}_{i,k}^{u,e} = \rho_u \frac{\left| (\mathbf{h}_{i,i,k}^e)^H \mathbf{h}_{i,i,k}^e \right|^2}{\left| \mu_{i,k}^{u,e} \right|^2 + \left| \eta_{i,k}^{u,e} \right|^2} \quad (38)$$

and the achievable UL rate can be calculated as  $\bar{C}_{i,k}^{u,e} = (1 - (K_{SPR}/K_{CS})\mu) \text{E}\{\log_2(1 + \overline{\text{SINR}}_{i,k}^{u,e})\}$ . Note that, unlike the result of the conventional scheme given in (6),  $\overline{\text{SINR}}_{i,k}^{u,e}$  increases as  $M$  increases, and in the asymptotic case of  $M \rightarrow \infty$ , we have  $\overline{\text{SINR}}_{i,k}^{u,e} \rightarrow \infty$ .

In summary, in contrast to the conventional scheme, which is unable to remove the PC by simply increasing the number of antennas at the BS  $M$ , for the edge users, we eliminated the PC imposed on the UL data transmission, and consequently, the UL achievable rate is significantly improved. Similar results can be obtained if we adopt the ZF detector for UL transmission in our proposal, and the ZF detector outperforms the MF detector, which will be verified by our numerical results.

### C. Downlink Transmission

Similar to the analysis of the UL transmission, here, we focus our attention on the DL transmission of the edge users in our proposal.

By adopting the MFMBD precoding matrix as derived in (29), the received signal vector of the  $K_{i,e}$  edge users in the  $i$ th cell can be represented as

$$\begin{aligned} \bar{\mathbf{y}}_i^{d,e} &= \sqrt{\rho_d} \sum_{j=1}^L (\mathbf{H}_{j,i}^e)^T \mathbf{W}_j^{\text{MFMBD}} \begin{bmatrix} \mathbf{x}_j^{d,c} \\ \mathbf{x}_j^{d,e} \end{bmatrix} + \bar{\mathbf{n}}_i^{d,e} \\ &= \sqrt{\rho_d} \sum_{j=1}^L \frac{1}{\sqrt{\gamma_j^{\text{MFMBD}}}} (\mathbf{H}_{j,i}^e)^T \mathbf{B}_j \mathbf{B}_j^\dagger \hat{\mathbf{H}}_{j,j}^* \begin{bmatrix} \mathbf{x}_j^{d,c} \\ \mathbf{x}_j^{d,e} \end{bmatrix} + \bar{\mathbf{n}}_i^{d,e} \\ &\approx \sqrt{\frac{\rho_d}{\gamma_i^{\text{MFMBD}}}} (\mathbf{H}_{i,i}^e)^T \mathbf{B}_i \mathbf{B}_i^\dagger \hat{\mathbf{H}}_{i,i}^* \begin{bmatrix} \mathbf{x}_i^{d,c} \\ \mathbf{x}_i^{d,e} \end{bmatrix} + \bar{\mathbf{n}}_i^{d,e} \end{aligned} \quad (39)$$

where  $\mathbf{x}_j^{d,c} = [x_{j,1}^{d,c}, x_{j,2}^{d,c}, \dots, x_{j,K_{j,c}}^{d,c}]^T$  are the symbols transmitted to the  $K_{j,c}$  center users in the  $j$ th cell,  $\mathbf{x}_j^{d,e} = [x_{j,1}^{d,e}, x_{j,2}^{d,e}, \dots, x_{j,K_{j,e}}^{d,e}]^T$  are the symbols destined for the  $K_{j,e}$

edge users in the  $j$ th cell,  $\bar{\mathbf{n}}_i^{\text{d,e}} = [\bar{n}_{i,1}^{\text{d,e}}, \bar{n}_{i,2}^{\text{d,e}}, \dots, \bar{n}_{i,K_{i,e}}^{\text{d,e}}]^T$  denotes the corresponding DL AWGN vector, and the approximation  $\approx$  holds as we apply  $\hat{\mathbf{H}}_{j,i}^e \approx \mathbf{H}_{j,i}^e$  and  $(\hat{\mathbf{H}}_{j,i}^e)^T \mathbf{B}_j = \mathbf{0}$  for  $j \neq i$  [see (28)].

Thus, for the  $k$ th edge user in the  $i$ th cell, the received symbol can be represented as

$$\bar{y}_{i,k}^{\text{d,e}} \approx \sqrt{\frac{\rho_d}{\gamma_i^{\text{MFMBD}}}} (\mathbf{h}_{i,i,k}^e)^T \mathbf{B}_i \mathbf{B}_i^\dagger (\mathbf{h}_{i,i,k}^e)^* x_{i,k}^{\text{d,e}} + \mu_{i,k}^{\text{d,e}} + \bar{n}_{i,k}^{\text{d,e}} \quad (40)$$

where the intracell interference  $\mu_{i,k}^{\text{d,e}}$  is given by

$$\mu_{i,k}^{\text{d,e}} = \sqrt{\frac{\rho_d}{\gamma_i^{\text{MFMBD}}}} \left( \sum_{k'=1}^{K_{i,c}} (\mathbf{h}_{i,i,k'}^e)^T \mathbf{B}_i \mathbf{B}_i^\dagger (\mathbf{h}_{i,i,k'}^e)^* x_{i,k'}^{\text{d,c}} + \sum_{k' \neq k} (\mathbf{h}_{i,i,k'}^e)^T \mathbf{B}_i \mathbf{B}_i^\dagger (\mathbf{h}_{i,i,k'}^e)^* x_{i,k'}^{\text{d,e}} \right). \quad (41)$$

Both  $\bar{n}_{i,k}^{\text{d,e}}$  and  $\mu_{i,k}^{\text{d,e}}$  can be made arbitrarily small by increasing the number of antennas at the BS. The DL SINR of the  $k$ th edge user in the  $i$ th cell can be then calculated as

$$\overline{\text{SINR}}_{i,k}^{\text{d,e}} \approx \frac{\rho_d}{\gamma_i^{\text{MFMBD}}} \cdot \frac{\left| (\mathbf{h}_{i,i,k}^e)^T \mathbf{B}_i \mathbf{B}_i^\dagger (\mathbf{h}_{i,i,k}^e)^* \right|^2}{\left| \mu_{i,k}^{\text{d,e}} \right|^2 + \left| \bar{n}_{i,k}^{\text{d,e}} \right|^2} \quad (42)$$

and the achievable DL rate can be calculated as  $\bar{C}_{i,k}^{\text{d,e}} = (1 - (K_{\text{SPR}}/K_{\text{CS}})\mu) \mathbb{E}\{\log_2(1 + \overline{\text{SINR}}_{i,k}^{\text{d,e}})\}$ . In contrast to the result of the conventional scheme given in (7),  $\overline{\text{SINR}}_{i,k}^{\text{d,e}}$  increases as  $M$  increases and in the asymptotic case of  $M \rightarrow \infty$ ; hence, we have  $\overline{\text{SINR}}_{i,k}^{\text{d,e}} \rightarrow \infty$ .

It is clear that, for the edge users, the PC is eliminated by our proposed scheme during the DL data transmission, and additionally, both the ICI and the intracell interference imposed on these edge users have been reduced by the MBD scheme. Similar results can be obtained if we adopt the ZF-based MBD TPC matrix, i.e.,  $\mathbf{W}_i^{\text{ZFMBD}}$ , for DL transmission in our proposal.

Taking into account the extra pilot resource, the achievable DL rate of the edge users has been significantly improved, whereas that of the center users is slightly reduced. Moreover, the average UL and DL cell throughputs of the SPR- and MBD-assisted system will be confirmed later by our simulation study.

#### D. Computational Complexity

The computational complexity of implementing the MBD scheme at the BS for the edge users will be quantified in terms of the number of complex-valued multiplications required, which includes the following two main contributions.

1) For the SVD operator, the complexity is on the order of  $MK_e^2$ , which is denoted by  $\mathcal{O}(MK_e^2)$ , which allows us to calculate  $\hat{\mathbf{A}}_i = \mathbf{U}_i \Sigma_i \mathbf{V}_i^H$  by using the QR decomposition.

TABLE I  
BASIC SIMULATION PARAMETERS

Number of cells $L_{\text{total}}$	19
Number of antennas in BS $M$	$32 \leq M \leq 256$
Number of users in the $i$ -th cell $K_i$	$8 \leq K_i \leq 10$
Number of pilot resource $K_{\text{CS}}$	$K_{\text{CS}} = 10$
Threshold $\rho_i$ adjustment parameter $\lambda$	$0.05 \leq \lambda \leq 1$
Cell radius $R$	500 m
Average transmit power at users $\rho_p, \rho_u$	10 dBm
Average transmit power at BS $\rho_d$	12 dBm
Path loss exponent $\alpha$	3
Log normal shadowing fading $\sigma_{\text{shadow}}$	8 dB
Carrier frequency	2 GHz
System bandwidth	10 MHz
Thermal noise density	-174 dBm/Hz
Pilot overhead parameter $\mu$	$\mu = 0.1$
Minimum distance between user and BS	30 m

2) For the matrix pseudoinverse operation, the complexity is on the order of  $\mathcal{O}(MK_{\text{CS}}^2)$ , which allows us to generate the ZF-based MBD precoding matrix by using the Gram-Schmidt algorithm.

The total computational complexity of implementing the MBD scheme at the BS is therefore on the order of  $\mathcal{O}(M(K_e^2 + K_{\text{CS}}^2))$ , which is comparable with that of the conventional scheme, and it is within the computational capability of a typical state-of-the-art BS.

## VII. SIMULATION STUDY

We evaluated the performance of the proposed SPR and MBD schemes using a set of Monte Carlo simulations. A typical hexagonal cellular network of  $L_{\text{total}}$  cells was considered, where the BS of each cell employed  $M$  AEs, and the  $i$ th cell had  $K_i$  single-AE users [2], [25], [26]. The default values of the various parameters of this simulated hexagonal cellular network are summarized in Table I. The large-scale fading coefficient  $\beta_{i,j,k}$  was generated according to [2]

$$\beta_{i,j,k} = \frac{z_{i,j,k}}{(r_{i,j,k}/R)^\alpha} \quad (43)$$

where  $R$  denotes the cell radius, and  $\alpha$  is the path loss exponent, whereas  $r_{i,j,k}$  is the distance between the  $k$ th user in the  $j$ th cell and the BS in the  $i$ th cell, whereas  $z_{i,j,k}$  denotes the shadow fading factor, which obeys the log-normal distribution, i.e.,  $10 \log_{10}(z_{i,j,k})$  follows the zero-mean Gaussian distribution having a standard deviation of  $\sigma_{\text{shadow}}$ . The reuse factor of center pilot group  $\Phi_c$  is 1, i.e., it is reused in all  $L_{\text{total}}$  cells, whereas the reuse factor of edge sub pilot groups  $\Phi_e = [\Phi_{e,1}^T, \Phi_{e,2}^T, \dots, \Phi_{e,7}^T]^T$  is 7, i.e., the  $i$ th cell utilizes  $\Phi_{e, \text{mod}(i,7)+1}$ , and nonadjacent cells reuse the same edge sub pilot group. The locations of the users in each cell were all randomly generated in each trial. A particular simulation trial is shown in Fig. 6, where the red crosses and green dots in each cell denote the center users and edge users, respectively, which are classified by the BS based on the threshold  $\rho_i$  associated with the parameter  $\lambda = 0.1$ . As stated previously and shown in Fig. 6, the classification of center users and edge users is not based on their distance from the serving BS.

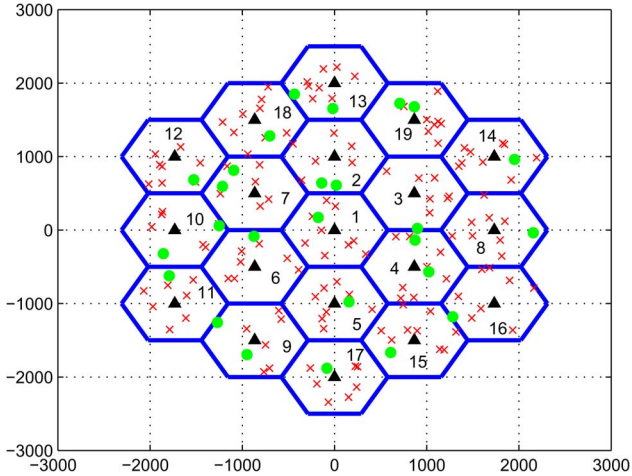


Fig. 6. Instantiation of the randomly generated user distribution in the simulated hexagonal cellular network, where red crosses, green dots, and black numbers denote center users, edge users, and cell numbers, respectively.

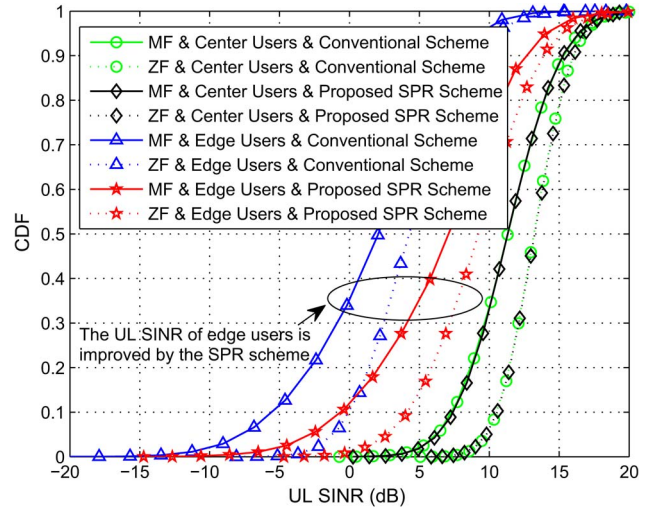


Fig. 8. CDF of UL SINR for the conventional and proposed SPR schemes with  $M = 128$  and  $\lambda = 0.1$ .

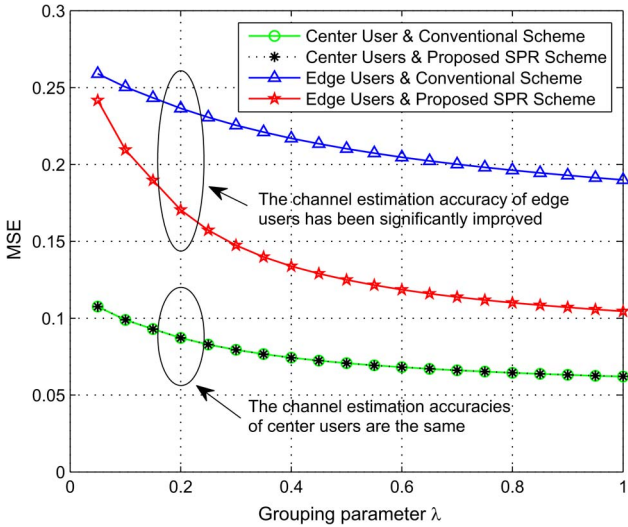


Fig. 7. Channel estimation accuracy comparison for the conventional and proposed SPR schemes with  $M = 128$ .

Fig. 7 compares the channel estimation accuracies as functions of the grouping parameter  $\lambda$  for both the conventional and proposed SPR schemes with  $M = 128$ . In each simulation trial, the channel estimation mean square error (MSE) of the edge users is calculated as

$$\text{MSE}^e = \text{E} \left\{ \frac{1}{K_e} \sum_{i=1}^L \sum_{k=1}^{K_{i,e}} \frac{\|\hat{\mathbf{h}}_{i,i,k}^e - \mathbf{h}_{i,i,k}^e\|_2^2}{\|\mathbf{h}_{i,i,k}^e\|_2^2} \right\} \quad (44)$$

where  $\hat{\mathbf{h}}_{i,i,k}^e$  denotes the estimate of the true channel vector  $\mathbf{h}_{i,i,k}^e$ , whereas the MSE of the channel estimation for the center users is defined as

$$\text{MSE}^c = \text{E} \left\{ \frac{1}{\left( \sum_{i=1}^L K_i \right) - K_e} \sum_{i=1}^L \sum_{k=1}^{K_{i,c}} \frac{\|\hat{\mathbf{h}}_{i,i,k}^c - \mathbf{h}_{i,i,k}^c\|_2^2}{\|\mathbf{h}_{i,i,k}^c\|_2^2} \right\} \quad (45)$$

where  $\hat{\mathbf{h}}_{i,i,k}^c$  denotes the estimate of the true channel vector  $\mathbf{h}_{i,i,k}^c$ . The average results over 100 random simulation runs are presented in Fig. 7. By increasing the grouping parameter  $\lambda$ , more users will be regarded as edge users. As expected, for the center users, who only suffer from a slight PC, both the conventional and proposed SPR schemes attain the same excellent channel estimation accuracy. However, the conventional scheme attains a poor channel estimation accuracy for the edge users, who suffer from severe PC. By contrast, since the PC is eliminated by applying orthogonal pilot sequences for the edge users in the adjacent cells, the channel estimation accuracy achieved by the proposed SPR scheme is significantly improved.

Fig. 8 shows the cumulative density function (CDF) of UL SINR for both the conventional and proposed SPR schemes with  $M = 128$  and  $\lambda = 0.1$ , where the results are presented by 1000 random simulation trials. In each simulation run, the conventional scheme calculates the UL SINR of a center or an edge user according to the first line of (5). For our SPR scheme, the UL SINR of center users is similar to that for the conventional scheme, whereas the UL SINR of edge users is calculated by the first line of (36) in each simulation trial. Since the UL transmission of the proposed SPR scheme is almost the same as that of the conventional scheme for the center users, their curves in Fig. 8 are almost coincided. Observed in Fig. 8, our SPR scheme attains a significantly higher UL SINR for the edge users than the conventional scheme. Furthermore, the ZF detector is always better than the MF detector by about 2 dB for both center users and edge users.

Fig. 9 shows the CDF of UL achievable rate for the conventional and proposed SPR schemes with  $M = 128$  and  $\lambda = 0.1$ , where the results are obtained from 500 random simulation runs. In each simulation trial, we generate the user positions first and then generate the channels of users for 50 times to obtain the UL achievable rate. Although the UL SINR results of the center users of the conventional and SPR schemes are the same as shown in Fig. 8, the UL achievable rates

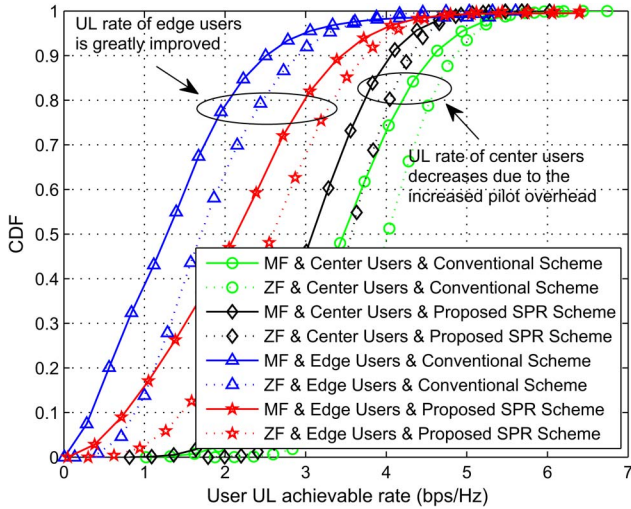


Fig. 9. CDF of UL achievable rate for the conventional and proposed SPR schemes with  $M = 128$  and  $\lambda = 0.1$ .

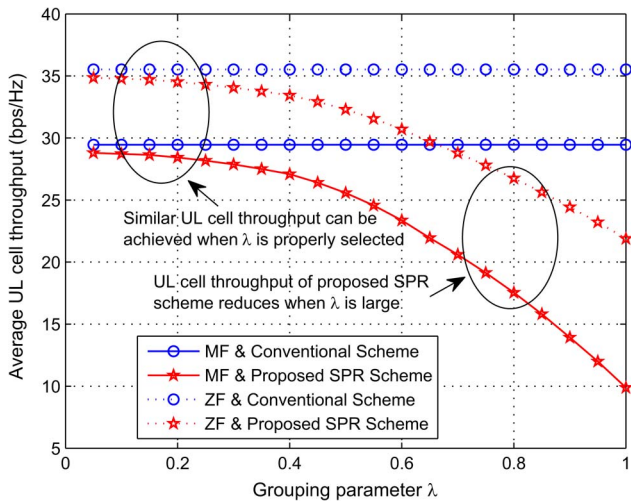


Fig. 10. Average UL cell throughput for the conventional and proposed SPR schemes with  $M = 128$  against  $\lambda$ .

are different due to the different pilot overheads, i.e.,  $\mu \rightarrow (K_{SPR}/K_{CS})\mu$ . It is clear that the UL achievable rate of edge users is significantly improved by the SPR scheme, whereas the UL achievable rate of center users decreases due to the increased pilot overhead. Moreover, the ZF detector always outperforms the MF detector by about 0.3 b/s/Hz per user.

Fig. 10 shows the average UL cell throughput for the conventional and proposed SPR schemes with  $M = 128$ . It is clear that, by increasing the group parameter  $\lambda$ , there will be more users regarded as edge users, which leads to the increase of pilot overhead and the decrease of UL achievable rate of center users. Thus, the proper selection of grouping parameter is important, e.g.,  $\lambda \leq 0.2$ , which improves the performance of edge users and ensures the cell throughput. Otherwise, e.g.,  $\lambda > 0.5$ , it is clear that the loss caused by overlarge pilot overhead outweighs the gain of the SPR scheme. In addition, the ZF detector always provides a gain about 5 b/s/Hz of average cell throughput compared with the MF detector.

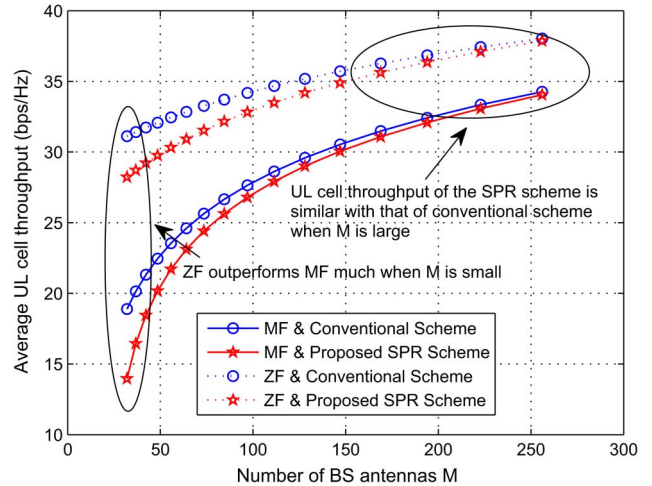


Fig. 11. Average UL cell throughput for the conventional and proposed SPR schemes with  $\lambda = 0.1$  against  $M$ .

Fig. 11 shows the average UL cell throughput comparison of the conventional and proposed SPR schemes with  $\lambda = 0.1$  against the number of BS antennas  $M$ . When the number of BS antennas is small, i.e.,  $M = 32$ , the average UL cell throughput of the proposed SPR scheme is smaller than that of the conventional scheme about 5 b/s/Hz with MF detector adopted. It is obvious that, to obtain the performance gain for edge users as shown in Fig. 9, the proposed SPR scheme sacrifices the spectral efficiency due to the increased pilot overhead and leads to the average UL cell throughput reduction. However, by increasing the number of BS antennas, e.g.,  $M = 256$ , it becomes clear that the average UL cell throughput of the proposed SPR scheme approaches that of the conventional scheme since the performance of edge users can be significantly improved by increasing  $M$ . Moreover, the ZF detector outperforms the MF detector a lot when  $M$  is small, and the gap shrinks as  $M$  increases.

Fig. 12 shows the CDF of DL achievable rate for the conventional system, the SPR-aided system, and the SPR- and MBD-assisted system with  $M = 128$  and  $\lambda = 0.1$ . Despite the MBD precoding scheme, it is clear that the results of DL achievable rate are similar with that of UL achievable rate, as shown in Fig. 9, due to their duality property. When the MBD precoding is considered, we find that the DL achievable rate of edge users can be significantly improved due to the elimination of the ICI, whereas the DL achievable rate of center users slightly decreases since the projecting operator of the MBD precoding sacrifices degrees of freedom of the DL signals for center users. Again, we can find that the ZFMBD precoding achieves a gain about 0.4 b/s/Hz compared with the MFMBD precoding for edge users.

Fig. 13 shows the average DL cell throughput for the conventional system, the SPR-aided system, and the SPR- and MBD-assisted system with  $\lambda = 0.1$  against  $M$ . The conventional system outperforms the SPR-aided system, whereas the SPR- and MBD-assisted system performs worst when small number of BS antennas is considered, e.g.,  $M = 32$ . However, considering the typical massive MIMO configuration as

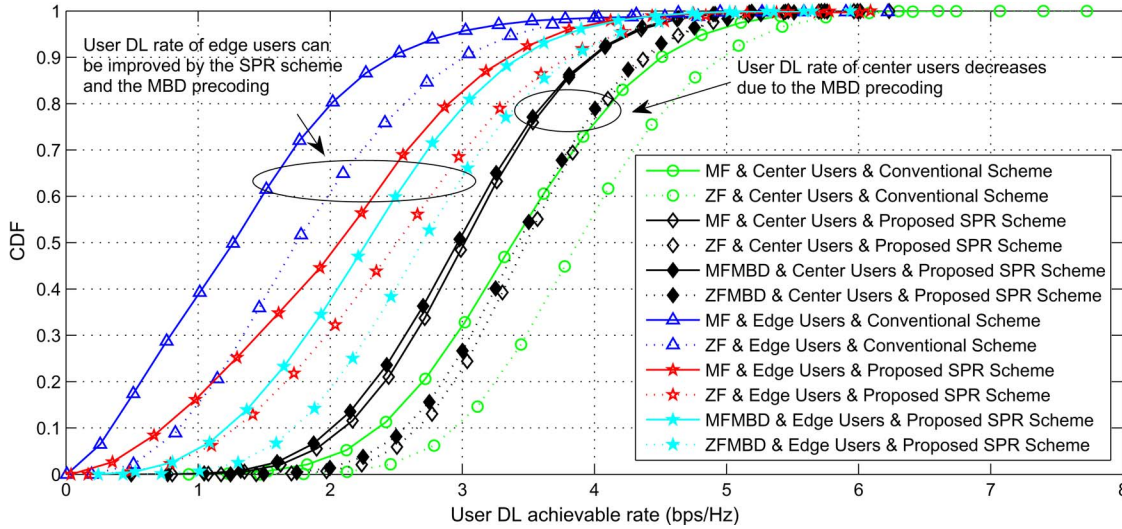


Fig. 12. CDF of DL achievable rate for the conventional system, the SPR-aided system, and the SPR- and MBD-assisted system with  $M = 128$  and  $\lambda = 0.1$ .

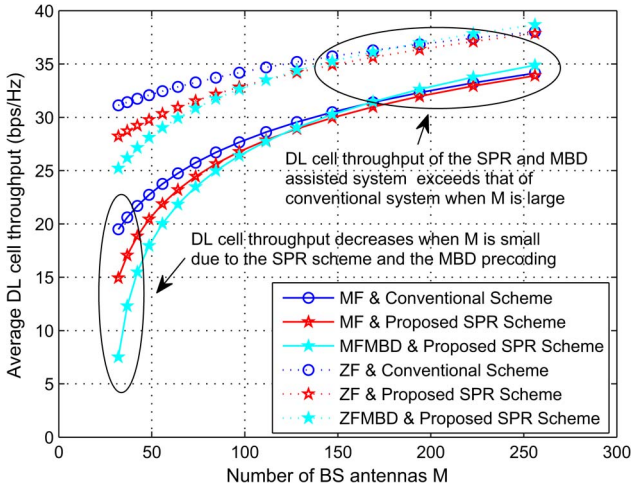


Fig. 13. Average DL cell throughput for the conventional system, the SPR-aided system, and the SPR- and MBD-assisted system with  $\lambda = 0.1$  against  $M$ .

$M = 256$ , it is clear that the average DL cell throughput of the SPR-aided system approaches that of the conventional scheme, and the SPR- and MBD-assisted system performs best among all three. Moreover, when  $M$  is further increased, the performance gap between the SPR- and MBD-assisted system and the conventional system will also become larger, which means that the increased rate of edge users becomes larger than the decreased rate of center users.

VIII. CONCLUSION

We have developed an SPR and MBD precoding regime for LS-MIMO systems, which are capable of significantly enhancing both the achievable UL and DL rates for edge users. Our contribution is twofold. First, we break away from the traditional practice of treating all users as though they suffer from the same level of PC and propose a simple yet effective means of dividing the users into cell-center and cell-edge users.

This grouping allows us to apply the proposed SPR scheme, whereby a center pilot group is reused for the center users in all cells, whereas the edge pilot group is applied to the edge users in the adjacent cells. By requiring a slightly increased number of pilot sequences, the proposed SPR scheme eliminates the PC inflicted upon the edge users who would otherwise suffer from severe PC in the conventional scheme. This significantly enhances the QoS for the edge users and, at the same time, ensures both the average UL and DL cell throughputs with slight and negligible reduction compared with that of the conventional system. Second, we further exploit the fact that the BS becomes capable of estimating the intercell channels of the edge users in the adjacent cells with the aid of the SPR regime without the deleterious effects of PC. Finally, we extend the classical BD precoding to a multicell scenario and propose the MBD precoding to eliminate the ICI imposed on the edge users of the adjacent cells in the DL. This MBD precoding further enhanced the performance of edge users in DL transmission and improved the average DL cell throughput, in addition to the gain obtained by the SPR scheme.

REFERENCES

- [1] T. L. Marzetta, "Noncooperative cellular wireless with unlimited numbers of base station antennas," *IEEE Trans. Wireless Commun.*, vol. 9, no. 11, pp. 3590–3600, Nov. 2010.
- [2] F. Rusek *et al.*, "Scaling up MIMO: Opportunities and challenges with very large arrays," *IEEE Signal Process. Mag.*, vol. 30, no. 1, pp. 40–60, Jan. 2013.
- [3] L. Lu, G. Y. Li, A. L. Swindlehurst, A. Ashikhmin, and R. Zhang, "An overview of massive MIMO: Benefits and challenges," *IEEE J. Sel. Top. Signal Process.*, vol. 8, no. 5, pp. 742–758, Oct. 2014.
- [4] H. Q. Ngo, E. G. Larsson, and T. L. Marzetta, "Energy and spectral efficiency of very large multiuser MIMO systems," *IEEE Trans. Commun.*, vol. 61, no. 4, pp. 1436–1449, Apr. 2013.
- [5] A. Goldsmith, S. A. Jafar, N. Jindal, and S. Vishwanath, "Capacity limits of MIMO channels," *IEEE J. Sel. Areas Commun.*, vol. 21, no. 5, pp. 684–702, Jun. 2003.
- [6] J. Jose, A. Ashikhmin, T. L. Marzetta, and S. Vishwanath, "Pilot contamination and precoding in multi-cell TDD systems," *IEEE Trans. Wireless Commun.*, vol. 10, no. 8, pp. 2640–2651, Aug. 2011.
- [7] F. Jin, R. Zhang, and L. Hanzo, "Frequency-swapping aided femtocells in twin-layer cellular networks relying on fractional frequency reuse," in *Proc. IEEE WCNC*, Apr. 1–4, 2012, pp. 3097–3101.

- [8] Y. Zhou *et al.*, "An overview on intercell interference management in mobile cellular networks: From 2G to 5G," in *Proc. IEEE ICCS*, Nov. 19–21, 2014, pp. 217–221.
- [9] L. Daewon *et al.*, "Coordinated multipoint transmission and reception in LTE-advanced: Deployment scenarios and operational challenges," *IEEE Commun. Mag.*, vol. 50, no. 2, pp. 148–155, Feb. 2012.
- [10] C. Junil, Z. Chance, D. J. Love, and U. Madhow, "Noncoherent trellis coded quantization: A practical limited feedback technique for massive MIMO systems," *IEEE Trans. Commun.*, vol. 61, no. 12, pp. 5016–5029, Dec. 2013.
- [11] K. Appaiah, A. Ashikhmin, and T. L. Marzetta, "Pilot contamination reduction in multi-user TDD systems," in *Proc. ICC*, Cape Town, South Africa, May 23–27, 2010, pp. 1–5.
- [12] F. Fernandes, A. Ashikhmin, and T. L. Marzetta, "Inter-cell interference in noncooperative TDD large scale antenna systems," *IEEE J. Sel. Areas Commun.*, vol. 31, no. 2, pp. 192–201, Feb. 2013.
- [13] H. Huh, S.-H. Moon, Y.-T. Kim, I. Lee, and G. Caire, "Multi-cell MIMO downlink with cell cooperation and fair scheduling: A large-system limit analysis," *IEEE Trans. Inf. Theory*, vol. 57, no. 12, pp. 7771–7786, Dec. 2011.
- [14] A. Ashikhmin and T. Marzetta, "Pilot contamination precoding in multi-cell large scale antenna systems," in *Proc. IEEE Int. Symp. Inf. Theory*, Cambridge, MA, USA, Jul. 1–6, 2012, pp. 1137–1141.
- [15] H. Q. Ngo and E. G. Larsson, "EVD-based channel estimation in multi-cell multiuser MIMO systems with very large antenna arrays," in *Proc. ICASSP*, Kyoto, Japan, Mar. 25–30, 2012, pp. 3249–3252.
- [16] H. Yin, D. Gesbert, M. Filippou, and Y. Liu, "A coordinated approach to channel estimation in large-scale multiple-antenna systems," *IEEE J. Sel. Areas Commun.*, vol. 31, no. 2, pp. 264–273, Feb. 2013.
- [17] H. Yin, D. Gesbert, M. Filippou, and Y. Liu, "Decontaminating pilots in massive MIMO systems," in *Proc. ICC*, Budapest, Hungary, Jun. 9–13, 2013, pp. 3170–3175.
- [18] J. Ma and P. Li, "Data-aided channel estimation in large antenna systems," *IEEE Trans. Signal Process.*, vol. 62, no. 12, pp. 3111–3124, Jun. 2014.
- [19] L. Cottatellucci, R. R. Muller, and M. Vehkaperä, "Analysis of pilot decontamination based on power control," in *Proc. VTC—Spring*, Dresden, Germany, Jun. 2–5, 2013, pp. 1–5.
- [20] R. R. Muller, L. Cottatellucci, and M. Vehkaperä, "Blind pilot decontamination," *IEEE J. Sel. Top. Signal Process.*, vol. 8, no. 5, pp. 773–786, Oct. 2014.
- [21] J. Zhang *et al.*, "Pilot contamination elimination for large-scale multiple-antenna aided OFDM systems," *IEEE J. Sel. Top. Signal Process.*, vol. 8, no. 5, pp. 759–772, Oct. 2014.
- [22] R. Persico, *The Singular Value Decomposition*. New York, NY, USA: Wiley, 2014.
- [23] Q. H. Spencer, A. L. Swindlehurst, and M. Haardt, "Zero-forcing methods for downlink spatial multiplexing in multiuser MIMO channels," *IEEE Trans. Signal Process.*, vol. 52, no. 2, pp. 461–471, Feb. 2004.
- [24] B. Hassibi and B. M. Hochwald, "How much training is needed in multiple-antenna wireless links?," *IEEE Trans. Inf. Theory*, vol. 49, no. 4, pp. 951–963, Apr. 2003.
- [25] Y. P. Seung, C. Junil, and D. J. Love, "Multicell cooperative scheduling for two-tier cellular networks," *IEEE Trans. Commun.*, vol. 62, no. 2, pp. 536–551, Feb. 2014.
- [26] Y. J. Hong, N. Lee, and B. Clerckx, "System level performance evaluation of inter-cell interference coordination schemes for heterogeneous networks in LTE-A system," in *Proc. IEEE GC Wkshps*, Dec. 6–10, 2010, pp. 690–694.



**Zhaocheng Wang** (M'09–SM'11) received the B.S., M.S., and Ph.D. degrees from Tsinghua University, Beijing, China, in 1991, 1993, and 1996, respectively.

From 1996 to 1997, he was a Postdoctoral Fellow with Nanyang Technological University, Singapore. From 1997 to 1999, he was with OKI Techno Centre (Singapore) Pte. Ltd., Singapore, where he was first a Research Engineer and later became a Senior Engineer. From 1999 to 2009, he was with Sony Deutschland GmbH, where he was first a Senior Engineer and later became a Principal Engineer. He is currently a Professor with the Department of Electronic Engineering, Tsinghua University. He has authored or coauthored over 80 SCI-indexed journal papers. He is the holder of 34 granted U.S./EU patents. His research areas include wireless communications, visible light communications, millimeter-wave communications, and digital broadcasting.

Prof. Wang is a Fellow of The Institution of Engineering and Technology. He has served as a Technical Program Committee Cochair of various international conferences.



**Chen Qian** received the B.S. degree from Tsinghua University, Beijing, China, in 2010. He is currently working toward the Ph.D. degree with the Broadband Communication and Signal Processing Laboratory, Tsinghua University.

His research areas include channel coding technology, multiple-input–multiple-output (MIMO) detection technology, and massive MIMO technology.



**Linglong Dai** (M'11–SM'14) received the B.S. degree from Zhejiang University, Hangzhou, China, in 2003; the M.S. degree (with the highest honor) from the China Academy of Telecommunications Technology, Beijing, China, in 2006; and the Ph.D. degree (with the highest honors) from Tsinghua University, Beijing, in 2011.

From 2011 to 2013, he was a Postdoctoral Fellow with the Department of Electronic Engineering, Tsinghua University, where he has been an Assistant Professor since July 2013. He has authored or coauthored over 50 journal and conference papers. His research interests are in wireless communications, with a focus on orthogonal frequency-division multiplexing, multiple-input–multiple-output, synchronization, channel estimation, multiple-access techniques, and wireless positioning.

Dr. Dai received the Outstanding Ph.D. Graduate of Tsinghua University in 2011, the Excellent Doctoral Dissertation of Beijing in 2012, the IEEE ICC Best Paper Award in 2013, the National Excellent Doctoral Dissertation Nomination Award in 2013, the IEEE ICC Best Paper Award in 2014, the URSI Young Scientists Award in 2014, and the IEEE Scott Helt Memorial Award in 2015 (IEEE TRANSACTIONS ON BROADCASTING Best Paper Award).



**Jinhui Chen** received the Ph.D. degree from Telecom ParisTech, Paris, France, in 2009.

From 2006 to 2009, she was a Research Assistant for Prof. D. T. M. Slock at EURECOM, Biot Sophia Antipolis, France. From 2009 to 2014, she was a Research Scientist with Alcatel-Lucent Bell Labs, Shanghai, China. Since 2014, she has been a Researcher and an Assistant Manager with Sony China Research Laboratory, Sony Corporation, Beijing, China. Her current research interests include multiple-input–multiple-output systems and wireless



**Xudong Zhu** received the B.S. degree from Tsinghua University, Beijing, China, in 2012. He is currently working toward the Ph.D. degree with the Broadband Communication and Signal Processing Laboratory, Tsinghua University.

His main research interests are in the areas of multiple-input–multiple-output (MIMO) technique and mobile communication, particularly in sparse signal reconstruction, massive MIMO, channel estimation, and precoding technique.

networks.



**Sheng Chen** (M'90–SM'97–F'08) received the B.Eng. degree in control engineering from East China Petroleum Institute, Dongying, China, in 1982; the Ph.D. degree in control engineering from City University London, London, U.K., in 1986; and the D.Sc. degree from the University of Southampton, Southampton, U.K., in 2005.

From 1986 to 1999, he held research and academic appointments with The University of Sheffield, Sheffield, U.K.; The University of Edinburgh, Edinburgh, U.K.; and the University of Portsmouth, Portsmouth, U.K. Since 1999, he has been with Electronics and Computer Science, University of Southampton, Southampton, U.K., where he is currently a Professor of intelligent systems and signal processing. He is also a Distinguished Adjunct Professor with King Abdulaziz University, Jeddah, Saudi Arabia. He has authored or coauthored over 500 research papers. He is an ISI highly cited researcher in engineering (March 2004). His research interests include adaptive signal processing, wireless communications, modeling and identification of nonlinear systems, neural network and machine learning, intelligent control system design, and evolutionary computation methods and optimization.

Dr. Chen is a Fellow of The Institution of Engineering and Technology. He was elected Fellow of the U.K. Royal Academy of Engineering in 2014.



**Lajos Hanzo** (M'91–SM'92–F'04) received the M.S. degree in electronics and the Ph.D. degree from the Technical University of Budapest, Budapest, Hungary, in 1976 and 1983, respectively; the D.Sc. degree from the University of Southampton, Southampton, U.K., in 2004; and the "Doctor Honoris Causa" degree from the Technical University of Budapest in 2009.

During his 38-year career in telecommunications, he has held various research and academic posts in Hungary, Germany, and the U.K. Since 1986, he has been with the School of Electronics and Computer Science, University of Southampton, where he holds the Chair in Telecommunications. He is currently directing an academic research team, working on a range of research projects in the field of wireless multimedia communications sponsored by industry, the Engineering and Physical Sciences Research Council (EPSRC), the European Research Council's Advanced Fellow Grant, and the Royal Society's Wolfson Research Merit Award. During 2008–2012, he was a Chaired Professor with Tsinghua University, Beijing, China. He is an enthusiastic supporter of industrial and academic liaison and offers a range of industrial courses. He has successfully supervised about 100 Ph.D. students, coauthored 20 John Wiley/IEEE Press books on mobile radio communications totaling in excess of 10 000 pages, and published more than 1400 research entries on IEEE Xplore.

Dr. Hanzo is a Fellow of the Royal Academy of Engineering, the Institution of Engineering and Technology, and the European Association for Signal Processing. He is also a Governor of the IEEE Vehicular Technology Society. During 2008–2012, he was the Editor-in-Chief of IEEE Press. He has served as the Technical Program Committee Chair and the General Chair of IEEE conferences, has presented keynote lectures, and has received a number of distinctions. His published work has more than 20 000 citations. Further information on research in progress and associated publications is available at <http://www-mobile.ecs.soton.ac.uk>.